

# MoMaStage: Skill-State Graph Guided Planning and Closed-Loop Execution for Long-Horizon Indoor Mobile Manipulation

Chenxu Li\*, Zixuan Chen\*, Yetao Li, Jiapeng Xu, Hongyu Ding, Jieqi Shi, Jing Huo, Yang Gao

**Abstract**—Indoor mobile manipulation (MoMA) enables robots to translate natural language instructions into physical actions, yet long-horizon execution remains challenging due to cascading errors and limited generalization across diverse environments. Learning-based approaches often fail to maintain logical consistency over extended horizons, while methods relying on explicit scene representations impose rigid structural assumptions that reduce adaptability in dynamic settings. To address these limitations, we propose MoMaStage, a structured vision-language framework for long-horizon MoMA that eliminates the need for explicit scene mapping. MoMaStage grounds a Vision-Language Model (VLM) within a Hierarchical Skill Library and a topology-aware Skill-State Graph, constraining task decomposition and skill composition within a feasible transition space. This structured grounding ensures that generated plans remain logically consistent and topologically valid with respect to the agent’s evolving physical state. To enhance robustness, MoMaStage incorporates a closed-loop execution mechanism that monitors proprioceptive feedback and triggers graph-constrained semantic replanning when deviations are detected, maintaining alignment between planned skills and physical outcomes. Extensive experiments in physics-rich simulations and real-world environments demonstrate that MoMaStage outperforms state-of-the-art baselines, achieving substantially higher planning success, reducing token overhead, and significantly improving overall task success rates in long-horizon mobile manipulation. Video demonstrations are available on the project website: <https://chenxuli-cxli.github.io/MoMaStage/>.

## I. INTRODUCTION

Indoor long-horizon mobile manipulation (MoMa) requires robots to accomplish tasks through extended sequences of navigation and object interaction within complex and dynamic environments such as homes and kitchens [1], [2]. These tasks tightly couple perception, decision-making, and control over long horizons while the agent interacts with changing environmental states. Although imitation learning approaches [3], [4], [5] have shown advantages over classical planning and control pipelines in terms of visual robustness and short-horizon dexterity, scaling these policies to long-horizon mobile manipulation remains challenging.

Long-horizon mobile manipulation is bottlenecked by the combinatorial explosion of task complexity. This increases expert data collection costs, limits the generalization of end-to-end policies [6], [7], and exacerbates compounding errors. While prior map-based symbolic planning methods [8], [9], [10], [11] attempt to address this, they are hindered by rigid assumptions, limited real-world semantic understanding, and computational overhead from explicit mapping.

\*Equal Contribution

All authors are with Nanjing University, China. Emails: {chenxuli, 241300010, 522025330117, hongyuding}@smail.nju.edu.cn, {chenzx, isjieqi, huojing, gaoy}@nju.edu.cn

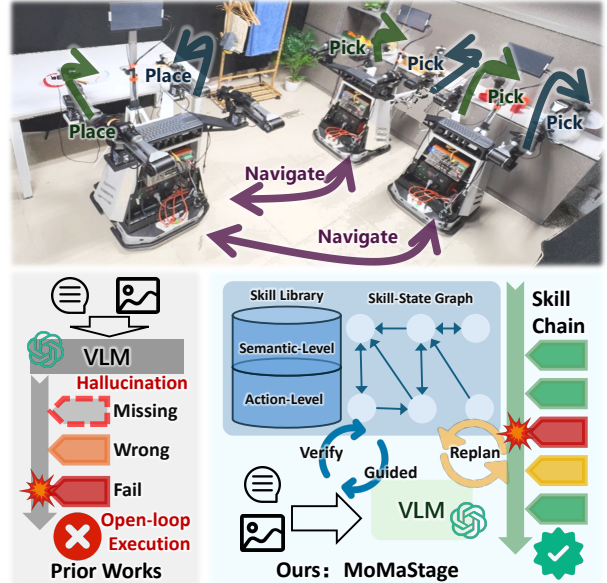


Fig. 1: We propose MoMaStage, a framework for long-horizon mobile manipulation that drives VLMs to translate instructions into valid skill chains via a Skill-State Graph and a hierarchical skill library, with closed-loop proprioceptive verification for guided replanning upon failure.

Recently, the integration of Vision-Language Models (VLMs) [12], [13], [14] has presented a highly promising alternative. These models possess vast internalized knowledge and demonstrate strong capabilities in grounding natural language instructions into sequential sub-tasks. However, purely VLM-driven agents often act without structural constraints. Frequently, open-loop language planners [15], [16], [17] may generate semantically plausible but physically inconsistent skill sequences. This is because executability depends not only on the current subtask, but also on the accumulated effects of previous skills which are often ignored by current methods [18], [19], [20].

To bridge this critical gap, we propose **MoMaStage**, a structured closed-loop framework driven by VLMs, designed for indoor long-horizon mobile manipulation without requiring explicit scene mapping, as shown in Figure 1. Our key insight is that, for long-horizon mobile manipulation, the critical missing abstraction is not a richer, explicit scene graph, but rather a state-grounded skill transition model that explicitly tracks how each semantic skill alters the robot-task state. Guided by this insight, our framework systematically constrains the generative reasoning of the VLM by

introducing a Hierarchical Skill Library and a topology-aware Skill-State Graph. Inspired by classical precondition-effect reasoning, we reformulate open-loop VLM planning into a state-grounded skill transition process. Unlike computationally heavy symbolic world models, our approach introduces a lightweight embodiment-state grounding interface that seamlessly embeds the robot’s evolving physical constraints directly into the structured graph.

Furthermore, executing long-horizon plans in the real world requires dynamic adaptability. To ensure robust execution, MoMaStage features a closed-loop mechanism that decouples physical safety from semantic reasoning. The system uses high-frequency proprioceptive ego-state monitoring to evaluate task progress and ensure immediate safety without inducing inference latency. Only when significant execution anomalies occur does it trigger semantic verification [21], [22], allowing the VLM to replan the skill sequence [18] and recover from out-of-distribution disruptions.

In summary, our primary contributions are as follows:

- We present MoMaStage, a map-free and VLM-driven framework for indoor long-horizon mobile manipulation, which unifies instruction understanding, skill-chain generation, execution, and feedback-driven refinement into a closed-loop decision-making pipeline.
- We introduce a state-grounded skill planning and execution mechanism built on a Skill-State Graph and a hierarchical skill library, which enforces cumulative state feasibility over VLM-generated skill chains and enables robust failure recovery through lightweight ego-state monitoring and targeted semantic replanning.
- We validate MoMaStage through extensive mobile manipulation experiments in complex simulations and dynamic real-world environments, demonstrating significant improvements in planning validity, execution robustness, and long-horizon task completion over representative baselines.

## II. RELATED WORK

### A. Mobile Manipulation and Skill Learning

Mobile manipulation has progressed from fixed-base tabletop settings toward household deployment and everyday activities [23]. Systems such as Mobile ALOHA [24] enable whole-body bimanual control, while HomeRobot [1] introduces the Open-Vocabulary Mobile Manipulation (OVMM) benchmark for pick-and-place in unseen environments, and OK-Robot [25] achieves zero-shot performance by composing open-knowledge models. At the policy level, large-scale VLA architectures, including RT-1 [6], RT-2 [12], VIMA [26], RoboAgent [27], Octo [7], OpenVLA [14], and DP-VLA [20], learn end-to-end language-conditioned policies, while imitation learning methods such as Implicit Behavioral Cloning [28], BeT [29], ACT [3], Diffusion Policy [4], UMI [30], and DP3 [5] provide visuomotor control. Furthermore, approaches like SPiRL [31] demonstrate the effectiveness of skill priors for accelerating downstream tasks. However, these monolithic policies struggle to maintain logical consistency over long horizons, as decisions

made at one stage often depend on latent state constraints accumulated from earlier interactions, making them brittle to error propagation.

### B. VLMs for Task Planning and Long-Horizon Execution

LLMs and VLMs have shown strong capabilities for task decomposition and semantic reasoning [15], [16], and reward-driven skill synthesis [32], [33]. They serve as zero-shot planners via code generation [34], PDDL representations [17], [11], or structured programs [35]. Embodied agents such as PaLM-E [13], DeCo [19], VoxPoser [36], and OWMM-Agent [2] integrate visual inputs with sequential sub-task generation, while ReAct [37] synergizes reasoning and acting. To ground these planners, SayPlan [9] leverages 3D scene graphs for large-scale LLM planning, and GRID [38] encodes scene graphs via graph attention networks to iteratively decompose instructions into sub-tasks. Recent work also explores execution-verifiable planning through specialized scene graphs [10]. Despite these advances, VLM-driven agents remain susceptible to physical hallucinations, often proposing invalid transitions that violate accumulated robot states.

### C. Closed-Loop Replanning and State Verification

Open-loop execution is brittle in dynamic environments. Classical TAMP [8] addresses this through rigorous state tracking, while learning-based frameworks such as Reflexion [39] and KnowNo [40] introduce verbal reinforcement and uncertainty quantification for failure handling. More recently, RePlan [18] uses a VLM to detect execution failures and triggers targeted replanning, while AHA [21] introduces a dedicated VLM fine-tuned to identify and explain manipulation errors, and frameworks like Code-as-Monitor [22] utilize constraint-aware visual programming for reactive failure detection. These approaches, however, rely on continuous or frequent VLM queries that incur significant inference latency, making them difficult to scale to long-horizon mobile manipulation, where timely feedback and lightweight recovery are essential.

## III. METHOD

In this section, we present the overall design of MoMaStage. As illustrated in Figure 2, the framework consists of three key modules designed to ensure logical feasibility, physical consistency, and execution robustness in long-horizon mobile manipulation. **1) Structured Skill Grounding.** We construct a Hierarchical Skill Library together with a Skill-State Graph to explicitly model skill preconditions and state transitions. This structured representation provides a formal grounding space that constrains high-level reasoning and prevents logically invalid skill compositions. **2) Graph-Constrained Planning and Verification.** Conditioned on the Skill Graph, the Vision-Language Model (VLM) decomposes natural language instructions into executable skill sequences. A post-hoc verification step based on the Skill-State Graph ensures that the generated plan satisfies global state consistency and transition feasibility. **3) Closed-Loop Execution**

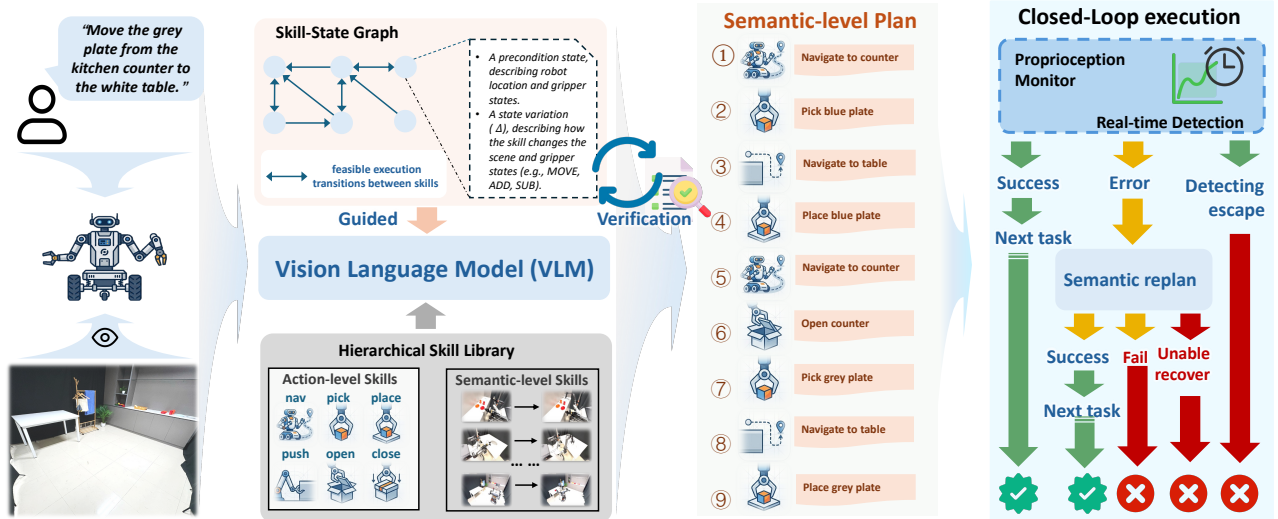


Fig. 2: **Overview of the MoMaStage framework.** Given multi-modal inputs, the system integrates **graph-constrained planning** with **closed-loop execution**. (a) The VLM-based planner decomposes long-horizon instructions into semantic skill sequences, restricted by the topological constraints of the *Skill Graph*. (b) A post-hoc feasibility check is performed using the *Skill-State Graph* to ensure global state consistency. (c) During execution, the system monitors ego-state transitions and triggers graph-grounded replanning to autonomously recover from failures (e.g., grasping or navigation errors).

**and Replanning.** During execution, the system continuously monitors ego-state transitions to detect deviations from expected outcomes. Upon failure, graph-grounded replanning is triggered to maintain logical validity and physical consistency throughout long-horizon task execution.

### A. Structured Skill Grounding

To systematically organize the agent’s capabilities and model their transition dynamics, we propose a structured representation comprising a Hierarchical Skill Library and an augmented Skill-State Graph.

1) *Hierarchical Skill Library*: The library  $\mathcal{S}$  is organized into two levels of granularity to balance execution flexibility and semantic reasoning:

**Action-Level Skills** ( $\mathcal{S}_{action}$ ): These fine-grained primitives (e.g., joint-level control, basic motion) are decoupled from scene semantics. They serve as foundational execution units yet lacking predefined execution orders.

**Semantic-Level Skills** ( $\mathcal{S}_{semantic}$ ): Tightly coupled with scene semantics, these skills possess explicit contextual preconditions and sequential relationships. A semantic skill is instantiated through end-to-end training, sequential composition of action primitives, or post-training refinement.

2) *Skill-State Graph*: We model the feasible transitions and state-transition dynamics among semantic skills via a Skill-State Graph  $\mathcal{G} = (\mathcal{V}, \mathcal{E})$ . Each node  $v_i \in \mathcal{V}$  represents a skill  $s_i \in \mathcal{S}_{semantic}$ , and a directed edge  $(v_i, v_j) \in \mathcal{E}$  denotes a feasible local transition. However, a purely topological graph is insufficient for stable long-horizon operations, as it only captures adjacent connectivity. In practice, skill executability depends on the cumulative embodiment state; for instance, a “pick” command is invalid if the gripper is already occupied, regardless of the topological adjacency.

To ensure state-traceable execution, we augment each node with a precondition state  $C$  and a state variation  $\Delta$ .

For a dual-arm mobile robot, the precondition state is a tuple:

$$C = (L_{scene}, O_{left}, O_{right}), \quad (1)$$

where  $L_{scene}$  denotes the robot’s location, and  $O_{left}, O_{right}$  denote objects held by the grippers ( $\emptyset$  for empty, underscore \_ for wildcard).

The resulting state variation induced by skill execution is mathematically formulated as:

$$\Delta = (f_{scene}, f_{left}, f_{right}). \quad (2)$$

The transformation functions are defined by the following operations:

- **Navigation**:  $f_{scene}$  applies  $MOVE(A, B)$  to transition the base from location  $A$  to  $B$ , or  $\emptyset$  for no displacement.
- **Manipulation**:  $f_{left}$  and  $f_{right}$  utilize  $ADD(a)$  to transition a gripper from  $\emptyset$  to object  $a$  (requiring an empty initial state), and  $SUB(a)$  to reset a gripper from  $a$  to  $\emptyset$  (requiring the object  $a$  to be present). An  $\emptyset$  operation indicates no state change.

By recursively applying  $\Delta$  to the initial state  $C$  along a proposed edge sequence, the system can dynamically verify global state consistency. Importantly, the proposed Skill-State Graph is not intended to be a full symbolic world model. Instead, it serves as a lightweight execution-consistency interface between high-level VLM reasoning and embodied skill execution. By only modeling the state variables that are most critical to long-horizon executability, our design preserves sufficient structure to reject invalid plans while avoiding the engineering overhead and brittleness of full scene-level symbolic reconstruction.

### B. Graph-Guided Planning and Verification

Given a long-horizon natural language instruction  $I$  and the current visual observation  $O_{vis}$ , our objective is to generate

a semantic skill sequence  $\mathbf{s} = [s_1, s_2, \dots, s_T]$  that maximizes task-consistent likelihood under the VLM planning while satisfying graph connectivity and cumulative state feasibility. We propose a two-stage framework: **topology-aware semantic planning** followed by **state-driven logical verification**.

1) *Topology-Aware Semantic Planning*: We formulate task decomposition as a structural routing problem over the skill space, guided by a multimodal reasoning engine. Rather than treating the Vision-Language Model (VLM) as a black-box planner, we constrain its reasoning within the feasible transitions defined by the Skill-State Graph.

The reasoning engine operates on three primary inputs: the instruction  $I$ , the visual observation  $O_{vis}$ , and a topological subgraph  $\mathcal{G}_{topo} \subset \mathcal{G}$ . Notably,  $\mathcal{G}_{topo}$  contains only the skill nodes and their adjacency relationships, omitting state-level attributes ( $C$  and  $\Delta$ ). By withholding explicit 3D scene models and symbolic object descriptions, we force the model to rely on the environmental affordances and robot capabilities encapsulated in the graph’s connectivity. Conditioned on these inputs, the VLM parses the high-level task into a candidate skill sequence  $\hat{\mathbf{s}} = [\hat{s}_1, \hat{s}_2, \dots, \hat{s}_K]$ , representing a topologically valid path through the skill space.

2) *State-Driven Feasibility Verification*: Once a candidate sequence  $\hat{\mathbf{s}}$  is generated, we perform a post-hoc verification using the full attributes of the Skill-State Graph to ensure long-horizon consistency. This stage transcends local adjacency by evaluating the cumulative state-transition chain.

Starting from the initial robot state  $C_0$ , the system recursively applies the state variation  $\Delta_i$  of each skill  $\hat{s}_i$  to compute the subsequent state  $C_{i+1}$ . A candidate plan is deemed feasible if and only if:

$$\forall i \in \{1, \dots, K\}, \text{is\_compatible}(C_{i-1}, \text{precondition}(\hat{s}_i)) \quad (3)$$

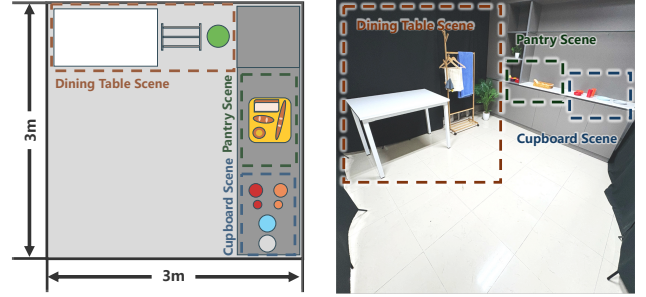
where the compatibility check ensures that gripper states ( $O_{left}, O_{right}$ ) and location constraints ( $L_{scene}$ ) satisfy the skill’s preconditions. If a state conflict is detected—such as attempting a “pick” operation while the gripper is occupied—the plan is rejected, and the system triggers a re-decomposition or adjustment within the VLM, ensuring the final output  $\mathbf{s}$  is both topologically and logically sound.

### C. Closed-Loop Execution and Replanning

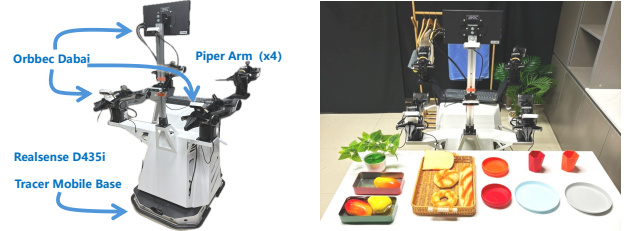
To ensure robust task completion in dynamic and uncertain environments, we implement a closed-loop execution mechanism. This stage integrates real-time state monitoring with graph-constrained recovery, enabling the agent to adaptively respond to execution deviations.

1) *State-Aware Execution Monitoring*: During the execution of the validated skill sequence  $\mathbf{s}$ , the system performs continuous state verification to ensure alignment between the physical environment and the planned logic. For each skill  $s_i$ , we employ a dual-layered monitoring process:

- **Ego-State Monitoring**: Tracks the robot’s proprioceptive data (e.g., joint encoders and gripper tactile sensors) to confirm the physical success of primitive actions, such as ensuring an object is successfully grasped (*ADD*) or released (*SUB*).



(a) Top-down schematic of the scene layout. (b) Photograph of the actual scene configuration.



(c) Hardware configuration of the robotic platform. (d) Objects and furniture involved in the experiments.

Fig. 3: Overview of the real-world experimental setup.

- **Semantic Verification**: Utilizes the VLM to perform post-execution scene checks, verifying that the environmental state matches the expected state variation  $\Delta_i$ .

If the observed state  $C_{obs}$  satisfies the expected outcome defined by  $\Delta_i$ , the agent proceeds to the next skill  $s_{i+1}$ . Otherwise, an execution deviation is flagged.

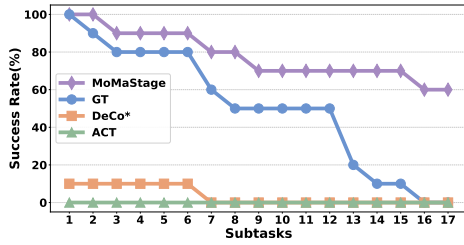
2) *Graph-Constrained Dynamic Replanning*: When a deviation or failure is detected (e.g., a pick failure or a blocked navigation path), MoMaStage does not simply restart the task. Instead, it triggers a dynamic replanning process anchored in the Skill-State Graph  $\mathcal{G}$ .

The current state  $C_{obs}$  is designated as the initial state. The system then performs a localized search or re-queries the VLM-based planner to identify a corrective path in  $\mathcal{G}$  that can transition the robot from  $C_{obs}$  to a state that satisfies the preconditions of the remaining sub-tasks. By leveraging the Skill-State Graph as the search space for replanning, the system ensures that the recovered sequence remains logically consistent and respects physical embodiment constraints. This graph-grounded feedback loop enables the agent to recover from failures autonomously, maintaining high success rates in long-horizon mobile manipulation tasks.

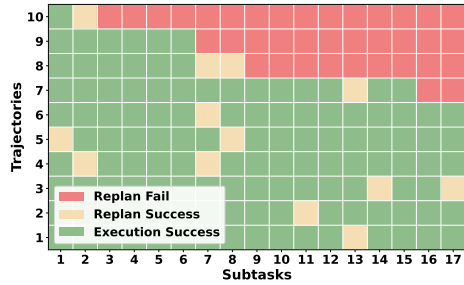
## IV. EXPERIMENTS

To evaluate the effectiveness of our proposed framework, MoMaStage, we conduct comprehensive experiments in both real-world environments and a simulated benchmark. Specifically, we address the following research questions:

- 1) Can MoMaStage be effectively deployed in real-world long-horizon mobile manipulation tasks, and does its closed-loop replanning mechanism effectively mitigate compounding execution errors compared to existing baselines?
- 2) How



(a) Success rates for methods.



(b) Detailed execution states of 10 trajectories.



(c) Qualitative visualization of a successful trajectory execution, highlighting the replanning capability to recover from a failure during subtask 7.

Fig. 4: Quantitative and qualitative evaluation of MoMaStage on the real-world robot platform. (a) MoMaStage maintains a higher success rate over long-horizon subtasks compared to baselines. (b) Trajectory-level execution details showing the system’s robustness through successful replanning. (c) A step-by-step demonstration of a long-horizon task, illustrating adaptive replanning when unexpected failures occur.

robust is the framework’s planning capability across diverse simulated environments, and how do different low-level skill configurations influence overall long-horizon execution success? 3) How does explicit topological grounding via the Skill-State Graph contribute to planning efficiency, and what do failure analyses reveal about the boundaries between high-level semantic reasoning and low-level physical limitations?

#### A. Experimental Setup

**Real-World Setup.** Experiments are conducted in a 3×3 m workspace divided into *Cupboard*, *Dining table*, and *Pantry* scenes (Figure 3). This segmentation is purely illustrative, as no environmental mapping is performed. We deploy our framework on the Agilex Cobot Magic platform, featuring four Agilex Piper arms and a Tracer mobile base. For multi-view observations, the robot uses four cameras: three Orbbec Dabai cameras (two wrist-mounted, one overhead) for manipulation, and an Intel RealSense D435i for both manipulation and navigation. The Skill-State Graph includes 16 semantic-level skills (6 pick, 6 place, 4 navigation) and 10 action-level skills for failure recovery. Semantic manipulation skills are trained using ACT on 50 spatially generalized demonstration trajectories, while navigation and action-level skills rely on predefined rules. We design 100 different long-horizon tasks consisting of different number of sub-tasks, involving frequent navigation-manipulation alternations and dual-arm coordination. Our goal is not to benchmark scene diversity but to evaluate whether the state-grounded planning and replanning mechanism can maintain consistency over extended execution horizons.

**Simulation Setup.** Experiments are conducted on *mshab\**, an extension of the ManiSkill-Hab benchmark [41]. We

evaluate across three original scenes: *tidy\_house* (4 stages, 20 subtasks), *prepare\_groceries* (3 stages, 12 subtasks), and *set\_table* (2 stages, 16 subtasks). Retaining original open-source weights, low-level skills employ Soft Actor-Critic (SAC) [42] and Behavior Cloning (BC) [43] for pick and place, Proximal Policy Optimization (PPO) [44] and BC for open and close, and PPO for navigation. To better align with our experimental objectives, *mshab\** introduces three critical modifications: (1) integrating a VLM interface for task decomposition and skill composition, integrating a VLM interface for task decomposition and skill composition, along with modules for task generation and translating planned skills into simulation-executable APIs; (2) enabling the seamless chaining of heterogeneous skill types, relaxing the previous single-skill-type restriction; and (3) supporting dynamic failure recovery by altering the skill execution sequence directly at the step of interruption.

**Baseline Models.** We compare MoMaStage with representative baselines in both simulation and real-world settings. *Ground Truth (GT) Sequencing* executes a human-authored optimal skill sequence without replanning or retry, serving as an execution upper bound and isolating physical execution from high-level VLM planning. *DeCo\** is an adapted version of the recent DeCo framework [19], modified to support our mobile manipulation setting and evaluated in both domains. We adopt DeCo as the primary planning baseline because it represents a recent VLM-driven skill decomposition approach without relying on heavy 3D scene representations. In contrast, methods such as VoxPoser [36] and SayPlan [9] depend on explicit spatial maps or benchmark-specific infrastructures, making direct comparison under our lightweight,

TABLE I: Performance Results (Mean  $\pm$  Standard Deviation)

Methods	Tidy_House			Prepare_Groceries			Set_Table		
	BC	RL	RL_Per_Obj	BC	RL	RL_Per_Obj	BC	RL	RL_Per_Obj
DeCo*	44.00 $\pm$ 3.74	46.67 $\pm$ 4.50	37.00 $\pm$ 4.55	35.00 $\pm$ 3.56	26.67 $\pm$ 3.68	25.67 $\pm$ 0.94	23.67 $\pm$ 2.49	20.33 $\pm$ 1.70	22.00 $\pm$ 2.16
<b>MoMaStage</b>	<b>80.67<math>\pm</math>2.87</b>	<b>85.67<math>\pm</math>3.09</b>	<b>79.67<math>\pm</math>4.11</b>	<b>90.33<math>\pm</math>2.05</b>	<b>85.67<math>\pm</math>4.11</b>	<b>91.67<math>\pm</math>2.62</b>	<b>93.67<math>\pm</math>1.25</b>	<b>87.00<math>\pm</math>5.10</b>	<b>91.00<math>\pm</math>2.16</b>

TABLE II: Consolidated Long-Horizon Subtask Success Rates (%)

Skill-State Graph Type	Methods	Tidy_House					Prepare_Groceries			Set_Table	
		Phase 1 (Step 4)	Phase 2 (Step 8)	Phase 3 (Step 12)	Phase 4 (Step 16)	Phase 5 (Step 20)	Phase 1 (Step 4)	Phase 2 (Step 8)	Phase 3 (Step 12)	Phase 1 (Step 8)	Phase 2 (Step 16)
RL_ALL (SAC+PPO)	GT	34.7 $\pm$ 2.1	10.0 $\pm$ 0.8	2.3 $\pm$ 0.5	0.3 $\pm$ 0.5	0.3 $\pm$ 0.5	19.7 $\pm$ 2.5	3.3 $\pm$ 0.5	0.0 $\pm$ 0.0	22.0 $\pm$ 1.6	0.0 $\pm$ 0.0
	DeCo*	13.7 $\pm$ 2.1	0.7 $\pm$ 0.5	0.0 $\pm$ 0.0	0.0 $\pm$ 0.0	0.0 $\pm$ 0.0	6.3 $\pm$ 1.3	0.0 $\pm$ 0.0	0.0 $\pm$ 0.0	4.0 $\pm$ 1.4	0.0 $\pm$ 0.0
	<b>MoMaStage</b>	<b>27.0 <math>\pm</math>1.4</b>	<b>12.3 <math>\pm</math>1.9</b>	<b>4.0 <math>\pm</math>0.0</b>	<b>1.7 <math>\pm</math>0.9</b>	<b>1.0 <math>\pm</math>0.0</b>	<b>17.7 <math>\pm</math>2.5</b>	<b>3.7 <math>\pm</math>1.7</b>	<b>0.0 <math>\pm</math>0.0</b>	<b>19.0 <math>\pm</math>0.0</b>	<b>0.0 <math>\pm</math>0.0</b>
IL_ALL + RL_ALL (BC+PPO)	GT	38.7 $\pm$ 2.9	9.0 $\pm$ 0.0	3.0 $\pm$ 0.8	0.3 $\pm$ 0.5	0.0 $\pm$ 0.0	14.0 $\pm$ 1.6	1.0 $\pm$ 0.8	0.0 $\pm$ 0.0	17.3 $\pm$ 1.7	0.0 $\pm$ 0.0
	DeCo*	18.3 $\pm$ 0.5	4.3 $\pm$ 1.2	0.3 $\pm$ 0.5	0.0 $\pm$ 0.0	0.0 $\pm$ 0.0	3.0 $\pm$ 0.8	0.0 $\pm$ 0.0	0.0 $\pm$ 0.0	2.7 $\pm$ 0.5	0.0 $\pm$ 0.0
	<b>MoMaStage</b>	<b>33.3 <math>\pm</math>2.6</b>	<b>7.0 <math>\pm</math>1.4</b>	<b>2.3 <math>\pm</math>0.9</b>	<b>1.0 <math>\pm</math>0.8</b>	<b>0.7 <math>\pm</math>0.5</b>	<b>11.3 <math>\pm</math>3.4</b>	<b>1.0 <math>\pm</math>0.8</b>	<b>0.7 <math>\pm</math>0.5</b>	<b>23.0 <math>\pm</math>1.4</b>	<b>0.0 <math>\pm</math>0.0</b>
RL_Per_Obj (SAC+PPO)	GT	41.3 $\pm$ 2.9	15.0 $\pm$ 2.2	3.6 $\pm$ 0.9	0.7 $\pm$ 0.9	0.7 $\pm$ 0.9	27.0 $\pm$ 0.8	2.3 $\pm$ 1.3	0.7 $\pm$ 0.9	25.3 $\pm$ 2.1	0.0 $\pm$ 0.0
	DeCo*	11.7 $\pm$ 0.5	4.0 $\pm$ 0.8	0.3 $\pm$ 0.5	0.0 $\pm$ 0.0	0.0 $\pm$ 0.0	6.7 $\pm$ 0.9	0.3 $\pm$ 0.5	0.3 $\pm$ 0.5	7.0 $\pm$ 1.4	0.0 $\pm$ 0.0
	<b>MoMaStage</b>	<b>31.7 <math>\pm</math>2.6</b>	<b>10.0 <math>\pm</math>2.2</b>	<b>4.7 <math>\pm</math>0.5</b>	<b>1.0 <math>\pm</math>0.8</b>	<b>1.0 <math>\pm</math>0.8</b>	<b>20.0 <math>\pm</math>1.6</b>	<b>2.3 <math>\pm</math>0.5</b>	<b>1.3 <math>\pm</math>0.5</b>	<b>27.3 <math>\pm</math>3.8</b>	<b>0.0 <math>\pm</math>0.0</b>

map-free mobile manipulation setup less appropriate. In real-world experiments, we additionally include *End-to-End ACT*, a non-modular learning baseline trained on 50 expert demonstrations of the full long-horizon task.

*B. Real-World Evaluation*

Due to space limitations, we report 10 tasks with the longest horizon (17 sub-tasks) in the main paper, which represents the most challenging long-horizon scenario involving cross-scene navigation and dual-arm manipulation. Results for tasks with shorter horizons are provided in the supplementary material.

Figure 4(a) tracks success rates across subtasks, where initial planning failures immediately terminate episodes to highlight long-horizon compounding challenges. Baselines struggle severely: **End-to-End ACT** fails instantly (0% success) due to covariate shift in imitation learning without modular decomposition. **DeCo\*** initiates only 10% of trials due to poor reasoning, dropping to 0% by subtask 7 lacking state verification and recovery strategies. Even **Ground Truth Sequencing**, despite perfect initial planning, steadily degrades to 0% by step 16 because its open-loop execution cannot recover from physical anomalies like grasping slips.

In stark contrast, **MoMaStage** achieves perfect initial planning and a 60% cumulative final success rate. Execution state tracking across the 10 trajectories in Figure 4(b) reveals this high survival rate stems from active closed-loop error correction rather than flawless execution. When encountering physical anomalies, the replanning module detects errors and synthesizes localized recovery actions, failing only in severe unrecoverable states like objects dropping out of the reachable workspace. Furthermore, Figure 4(c) qualitatively visualizes a successful trajectory, detailing the step-by-step execution and highlighting a crucial adaptive replanning moment at subtask 7 that seamlessly recovers from an unexpected failure to complete the long-horizon task.

*C. Simulation Benchmarking*

To evaluate our framework under diverse policy constraints, large-scale simulation experiments using Gemini

2.5 Flash as the reasoning engine are conducted across three complex scenes: *tidy.house*, *prepare.groceries*, and *set.table*. Pre-trained Behavior Cloning (BC) and Reinforcement Learning (RL) policies drive physical execution. To ensure statistical robustness, we comprehensively evaluate three methods (GT, DeCo\*, and MoMaStage) across all three scenes and their corresponding three Skill-State Graph configurations. For each specific setup, we execute 100 episodes across 3 independent trial groups to compute the mean and standard deviation, culminating in a rigorous total of 8,100 simulated trajectories.

1) *Planning Robustness Across Environments*: Table I details planning success rates. While the *DeCo\** baseline heavily struggles with multi-step reasoning—severely degrading in demanding tasks like *set.table*—our framework maintains exceptional reliability (79%–94%). Explicitly grounding the Vision-Language Model within the Skill-State Graph effectively eliminates logical hallucinations, generating valid sequences regardless of the underlying low-level policy.

2) *Long-Horizon Execution Attrition and Bottlenecks*: Despite robust planning, extended physical execution remains challenging. Table II tracks execution success at each sequential sub-phase across three Skill-State Graph configurations: *RL\_ALL*, *IL\_ALL + RL\_ALL*, and *RL\_Per\_Obj*, perfectly aligning with the predefined policy settings in the *mshab* benchmark.

Success rates drop significantly over 20-step horizons for all methods due to compounding errors. Notably, *MoMaStage* initially trails ground-truth (GT) sequencing, as early-stage performance is heavily bounded by initial planning success. However, open-loop GT degrades rapidly amidst physical anomalies, whereas *MoMaStage*’s closed-loop replanning effectively recovers from execution failures, surpassing GT in mid-to-late phases.

Comparing Skill-State Graphs reveals a design trade-off: *RL\_Per\_Obj* features robust, object-specific skills that increase cognitive burden, initially lowering planning success. Yet, its superior physical execution robustness compensates over time, outperforming generalized but physically brittle

skill sets. This underscores the necessity of balancing skill vocabulary size with individual skill capabilities.

### 3) Physical Limitations and Sim-to-Real Discrepancy:

Even optimal GT sequencing approaches a 0% success rate, proving the primary bottleneck is not semantic reasoning, but simulated low-level physical errors. Although the reasoning engine detects anomalies and proposes semantic recoveries, the simulated policies repeatedly fail to execute them. Contrasting this with our successful real-world replanning highlights limitations in standard simulation benchmarks, validating our algorithmic planning robustness while emphasizing the need for physically compliant low-level skills.

### D. Ablation Study and Failure Analysis

TABLE III: Planning Performance and Computational Cost Comparison. Metrics are reported as Mean  $\pm$  Standard Deviation across all trials.

Methods	Succ. (%) $\uparrow$	Time (s) $\downarrow$	Tokens $\downarrow$	Think. Tok. $\downarrow$
DeCo*	0.0 $\pm$ 0.0	21.4 $\pm$ 5.7	5814 $\pm$ 436	3853 $\pm$ 581
MoMaStage*	100.0 $\pm$ 0.0	24.6 $\pm$ 4.2	9106 $\pm$ 678	2927 $\pm$ 421
<b>MoMaStage</b>	<b>100.0</b> $\pm$ 0.0	<b>16.0</b> $\pm$ 1.1	<b>6633</b> $\pm$ 218	<b>2485</b> $\pm$ 230

TABLE IV: Failure Analysis

Scene	Graph	FLE(%)	TLE(%)	PTF(%)
<i>Tidy_House</i>	BC	83.7 $\pm$ 2.5	16.3 $\pm$ 2.5	0.0 $\pm$ 0.0
	RL	81.0 $\pm$ 3.0	19.0 $\pm$ 3.0	0.0 $\pm$ 0.0
	RL_Per_Obj	80.0 $\pm$ 5.0	20.0 $\pm$ 5.0	0.0 $\pm$ 0.0
<i>Prepare_Groceries</i>	BC	52.0 $\pm$ 5.6	48.0 $\pm$ 5.6	0.0 $\pm$ 0.0
	RL	59.3 $\pm$ 4.5	40.7 $\pm$ 4.5	0.0 $\pm$ 0.0
	RL_Per_Obj	52.3 $\pm$ 5.0	47.7 $\pm$ 5.0	0.0 $\pm$ 0.0
<i>Set_Table</i>	BC	72.7 $\pm$ 3.5	27.3 $\pm$ 3.5	0.0 $\pm$ 0.0
	RL	70.7 $\pm$ 1.5	29.3 $\pm$ 1.5	0.0 $\pm$ 0.0
	RL_Per_Obj	70.7 $\pm$ 4.7	29.3 $\pm$ 4.7	0.0 $\pm$ 0.0

To evaluate planning efficiency using Gemini 2.5 Flash, Table III summarizes performance across four metrics. The baseline DeCo\* completely fails (0% success) yet consumes excessive resources (averaging 3853 thinking tokens), indicating that without explicit topological constraints, the Vision-Language Model (VLM) wastes computational effort navigating invalid logical pathways.

Conversely, both MoMaStage variants achieve 100% planning success. However, MoMaStage\* supplies the VLM with the entire, unpruned Skill-State Graph, introducing redundant complexity. By explicitly extracting a focused Skill Graph based on state-driven constraints, the standard MoMaStage architecture drastically improves efficiency over MoMaStage\*, reducing inference time (24.6s to 16.0s), total tokens (9106 to 6633), and thinking tokens (2927 to 2485). This proves that guiding VLM reasoning via a structurally refined subgraph—rather than a monolithic state space—significantly alleviates cognitive load, maintaining perfect reliability while minimizing latency and API costs.

As detailed in Table I, benchmarking generalization across diverse scenes and policies further highlights this advantage. While *DeCo\** struggles with multi-step reasoning, plateauing between 20% and 47% and degrading in complex tasks like

*set\_table*, MoMaStage maintains robust success rates across all configurations. Grounding VLM planning within the Skill-State Graph bridges semantic reasoning and embodied execution for dependable long-horizon completion.

To isolate high-level reasoning from low-level physical limitations, Table IV categorizes execution failures into three terminal modes: *Force Limit Exceeded* (FLE), *Time Limit Exceeded* (TLE), and *Preceding Task Failed* (PTF).

Crucially, the majority of execution failures are FLE, stemming directly from simulation anomalies like mesh clipping and physics engine calculation bugs during intense manipulation. Originating from fundamentally flawed simulated physical states rather than semantic errors, these are logically unrecoverable by the high-level policy.

The remaining failures are TLE, occurring when a skill surpasses its time bound. Log analyses reveal this typically happens when objects drop or policies encounter Out-of-Distribution (OOD) states. For example, if an object slips during navigation without localized recovery primitives, the policy enters an infinite loop attempting to reach an unmanipulable target, causing a timeout.

Finally, PTF remains consistently at 0.0% across all configurations, proving the system never inadvertently undoes completed subtasks. This strict monotonic progression validates the efficacy of our rigorous state verification and closed-loop topological grounding.

## V. CONCLUSION

In this work, we present MoMaStage, a map-free, vision-language-driven framework for long-horizon indoor mobile manipulation. By introducing a state-grounded Skill-State Graph and a graph-constrained closed-loop execution mechanism, MoMaStage improves the logical validity and execution consistency of long-horizon skill chains for robust, real-time adaptation. Extensive real-world and simulated evaluations demonstrate that MoMaStage greatly reduces token costs, achieves substantially higher initial planning success, and significantly improves overall execution reliability, suggesting that explicitly modeling embodiment-state transitions is an effective way to bridge high-level semantic reasoning and long-horizon robot execution. Finally, as high-level reasoning is no longer the primary bottleneck, future work will focus on enhancing the physical dexterity of foundational action-level skills to bridge the gap between logical planning and robust physical embodiment.

## REFERENCES

- [1] S. Yenamandra, A. Ramachandran, K. Yadav, A. Wang, M. Khanna, T. Gervet, T.-Y. Yang, V. Jain, A. W. Clegg, J. Turner, *et al.*, "Homerobot: Open-vocabulary mobile manipulation," *arXiv preprint arXiv:2306.11565*, 2023.
- [2] J. Chen, H. Liang, L. Du, W. Wang, M. Hu, Y. Mu, W. Wang, J. Dai, P. Luo, W. Shao, *et al.*, "Owmm-agent: Open world mobile manipulation with multi-modal agentic data synthesis," *arXiv preprint arXiv:2506.04217*, 2025.
- [3] T. Z. Zhao, V. Kumar, S. Levine, and C. Finn, "Learning fine-grained bimanual manipulation with low-cost hardware," *arXiv preprint arXiv:2304.13705*, 2023.

- [4] C. Chi, Z. Xu, S. Feng, E. Cousineau, Y. Du, B. Burchfiel, R. Tedrake, and S. Song, "Diffusion policy: Visuomotor policy learning via action diffusion," *The International Journal of Robotics Research*, vol. 44, no. 10-11, pp. 1684–1704, 2025.
- [5] Y. Ze, G. Zhang, K. Zhang, C. Hu, M. Wang, and H. Xu, "3d diffusion policy: Generalizable visuomotor policy learning via simple 3d representations," *arXiv preprint arXiv:2403.03954*, 2024.
- [6] A. Brohan, N. Brown, J. Carbajal, Y. Chebotar, J. Dabis, C. Finn, K. Gopalakrishnan, K. Hausman, A. Herzog, J. Hsu, *et al.*, "Rt-1: Robotics transformer for real-world control at scale," *arXiv preprint arXiv:2212.06817*, 2022.
- [7] O. M. Team, D. Ghosh, H. Walke, K. Pertsch, K. Black, O. Mees, S. Dasari, J. Hejna, T. Kreiman, C. Xu, *et al.*, "Octo: An open-source generalist robot policy," *arXiv preprint arXiv:2405.12213*, 2024.
- [8] C. R. Garrett, R. Chitnis, R. Holladay, B. Kim, T. Silver, L. P. Kaelbling, and T. Lozano-Pérez, "Integrated task and motion planning," *Annual review of control, robotics, and autonomous systems*, vol. 4, no. 1, pp. 265–293, 2021.
- [9] K. Rana, J. Haviland, S. Garg, J. Abou-Chakra, I. Reid, and N. Suenderhauf, "Sayplan: Grounding large language models using 3d scene graphs for scalable robot task planning," *arXiv preprint arXiv:2307.06135*, 2023.
- [10] D. Ekpo, M. Levy, S. Suri, C. Huynh, and A. Shrivastava, "Verigraph: Scene graphs for execution verifiable robot planning," *arXiv preprint arXiv:2411.10446*, 2024.
- [11] H. Ye, Y. Xiao, C. Lu, and P. Cai, "Uniplan: Vision-language task planning for mobile manipulation with unified pddl formulation," *arXiv preprint arXiv:2602.08537*, 2026.
- [12] A. Brohan, N. Brown, J. Carbajal, Y. Chebotar, X. Chen, K. Chormanski, T. Ding, D. Driess, A. Dubey, C. Finn, *et al.*, "Rt-2: Vision-language-action models transfer web knowledge to robotic control, 2023," [URL https://arxiv.org/abs/2307.15818](https://arxiv.org/abs/2307.15818), vol. 1, p. 2, 2024.
- [13] D. Driess, F. Xia, M. S. Sajjadi, C. Lynch, A. Chowdhery, B. Ichter, A. Wahid, J. Tompson, Q. Vuong, T. Yu, *et al.*, "Palm-e: An embodied multimodal language model," *arXiv preprint arXiv:2303.03378*, 2023.
- [14] M. J. Kim, K. Pertsch, S. Karamcheti, T. Xiao, A. Balakrishna, S. Nair, R. Rafailov, E. Foster, G. Lam, P. Sanketi, *et al.*, "Openvla: An open-source vision-language-action model," *arXiv preprint arXiv:2406.09246*, 2024.
- [15] M. Ahn, A. Brohan, N. Brown, Y. Chebotar, O. Cortes, B. David, C. Finn, C. Fu, K. Gopalakrishnan, K. Hausman, *et al.*, "Do as i can, not as i say: Grounding language in robotic affordances," *arXiv preprint arXiv:2204.01691*, 2022.
- [16] W. Huang, F. Xia, T. Xiao, H. Chan, J. Liang, P. Florence, A. Zeng, J. Tompson, I. Mordatch, Y. Chebotar, *et al.*, "Inner monologue: Embodied reasoning through planning with language models," *arXiv preprint arXiv:2207.05608*, 2022.
- [17] B. Liu, Y. Jiang, X. Zhang, Q. Liu, S. Zhang, J. Biswas, and P. Stone, "Llm+ p: Empowering large language models with optimal planning proficiency," *arXiv preprint arXiv:2304.11477*, 2023.
- [18] M. Skreta, Z. Zhou, J. L. Yuan, K. Darvish, A. Aspuru-Guzik, and A. Garg, "Replan: Robotic replanning with perception and language models," *arXiv preprint arXiv:2401.04157*, 2024.
- [19] Z. Chen, J. Yin, Y. Chen, J. Huo, P. Tian, J. Shi, Y. Hou, Y. Li, and Y. Gao, "Deco: Task decomposition and skill composition for zero-shot generalization in long-horizon 3d manipulation," *IEEE Robotics and Automation Letters*, 2026.
- [20] B. Han, J. Kim, and J. Jang, "A dual process vla: Efficient robotic manipulation leveraging vlm," *arXiv preprint arXiv:2410.15549*, 2024.
- [21] J. Duan, W. Pumacay, N. Kumar, Y. R. Wang, S. Tian, W. Yuan, R. Krishna, D. Fox, A. Mandlekar, and Y. Guo, "Aha: A vision-language-model for detecting and reasoning over failures in robotic manipulation," *arXiv preprint arXiv:2410.00371*, 2024.
- [22] E. Zhou, Q. Su, C. Chi, Z. Zhang, Z. Wang, T. Huang, L. Sheng, and H. Wang, "Code-as-monitor: Constraint-aware visual programming for reactive and proactive robotic failure detection," in *Proceedings of the Computer Vision and Pattern Recognition Conference*, 2025, pp. 6919–6929.
- [23] S. Srivastava, C. Li, M. Lingelbach, R. Martín-Martín, F. Xia, K. E. Vainio, Z. Lian, C. Gokmen, S. Buch, K. Liu, *et al.*, "Behavior: Benchmark for everyday household activities in virtual, interactive, and ecological environments," in *Conference on robot learning*. PMLR, 2022, pp. 477–490.
- [24] Z. Fu, T. Z. Zhao, and C. Finn, "Mobile aloha: Learning bimanual mobile manipulation with low-cost whole-body teleoperation," *arXiv preprint arXiv:2401.02117*, 2024.
- [25] P. Liu, Y. Orru, J. Vakil, C. Paxton, N. M. M. Shafiullah, and L. Pinto, "Ok-robot: What really matters in integrating open-knowledge models for robotics," *arXiv preprint arXiv:2401.12202*, 2024.
- [26] Y. Zhu *et al.*, "Vima: General robot manipulation with multimodal prompts," in *International Conference on Learning Representations (ICLR)*, 2023.
- [27] H. Bharadhwaj, J. Vakil, M. Sharma, A. Gupta, S. Tulsiani, and V. Kumar, "Roboagent: Generalization and efficiency in robot manipulation via semantic augmentations and action chunking," in *2024 IEEE International Conference on Robotics and Automation (ICRA)*. IEEE, 2024, pp. 4788–4795.
- [28] P. Florence, C. Lynch, A. Zeng, O. A. Ramirez, A. Wahid, L. Downs, A. Wong, J. Lee, I. Mordatch, and J. Tompson, "Implicit behavioral cloning," in *Conference on robot learning*. PMLR, 2022, pp. 158–168.
- [29] N. M. Shafiullah, Z. Cui, A. A. Altanzaya, and L. Pinto, "Behavior transformers: Cloning  $k$  modes with one stone," *Advances in neural information processing systems*, vol. 35, pp. 22955–22968, 2022.
- [30] C. Chi, Z. Xu, C. Pan, E. Cousineau, B. Burchfiel, S. Feng, R. Tedrake, and S. Song, "Universal manipulation interface: In-the-wild robot teaching without in-the-wild robots," *arXiv preprint arXiv:2402.10329*, 2024.
- [31] K. Pertsch, Y. Lee, and J. Lim, "Accelerating reinforcement learning with learned skill priors," in *Conference on robot learning*. PMLR, 2021, pp. 188–204.
- [32] W. Yu, N. Gileadi, C. Fu, S. Kirmani, K.-H. Lee, M. G. Arenas, H.-T. L. Chiang, T. Erez, L. Hasenclever, J. Humprik, *et al.*, "Language to rewards for robotic skill synthesis," *arXiv preprint arXiv:2306.08647*, 2023.
- [33] Y. J. Ma, W. Liang, G. Wang, D.-A. Huang, O. Bastani, D. Jayaraman, Y. Zhu, L. Fan, and A. Anandkumar, "Eureka: Human-level reward design via coding large language models," *arXiv preprint arXiv:2310.12931*, 2023.
- [34] J. Liang, W. Huang, F. Xia, P. Xu, K. Hausman, B. Ichter, P. Florence, and A. Zeng, "Code as policies: Language model programs for embodied control," in *2023 IEEE International conference on robotics and automation (ICRA)*. IEEE, 2023, pp. 9493–9500.
- [35] I. Singh, V. Blukis, A. Mousavian, A. Goyal, D. Xu, J. Tremblay, D. Fox, J. Thomason, and A. Garg, "Progprompt: Generating situated robot task plans using large language models," *arXiv preprint arXiv:2209.11302*, 2022.
- [36] W. Huang, C. Wang, R. Zhang, Y. Li, J. Wu, and L. Fei-Fei, "Voxposer: Composable 3d value maps for robotic manipulation with language models," *arXiv preprint arXiv:2307.05973*, 2023.
- [37] S. Yao, J. Zhao, D. Yu, N. Du, I. Shafraan, K. R. Narasimhan, and Y. Cao, "React: Synergizing reasoning and acting in language models," in *The eleventh international conference on learning representations*, 2022.
- [38] Z. Ni, X. Deng, C. Tai, X. Zhu, Q. Xie, W. Huang, X. Wu, and L. Zeng, "Grid: Scene-graph-based instruction-driven robotic task planning," in *2024 IEEE/RSJ International Conference on Intelligent Robots and Systems (IROS)*. IEEE, 2024, pp. 13765–13772.
- [39] N. Shinn, F. Cassano, A. Gopinath, K. Narasimhan, and S. Yao, "Reflexion: Language agents with verbal reinforcement learning," *Advances in neural information processing systems*, vol. 36, pp. 8634–8652, 2023.
- [40] A. Z. Ren, A. Dixit, A. Bodrova, S. Singh, S. Tu, N. Brown, P. Xu, L. Takayama, F. Xia, J. Varley, *et al.*, "Robots that ask for help: Uncertainty alignment for large language model planners," *arXiv preprint arXiv:2307.01928*, 2023.
- [41] A. Shukla, S. Tao, and H. Su, "Maniskill-hab: A benchmark for low-level manipulation in home rearrangement tasks," *arXiv preprint arXiv:2412.13211*, 2024.
- [42] T. Haarnoja, A. Zhou, P. Abbeel, and S. Levine, "Soft actor-critic: Off-policy maximum entropy deep reinforcement learning with a stochastic actor," in *International conference on machine learning*. Pmlr, 2018, pp. 1861–1870.
- [43] M. Bain and C. Sammut, "A framework for behavioural cloning," in *Machine intelligence 15*, 1995, pp. 103–129.
- [44] J. Schulman, F. Wolski, P. Dhariwal, A. Radford, and O. Klimov, "Proximal policy optimization algorithms," *arXiv preprint arXiv:1707.06347*, 2017.